Assessing the Refractive Index of Glass Beads for Use in Road-marking Applications via Retroreflectance Measurement

Sang Yeol Shin[1], Ji In Lee[1], Woon Jin Chung[2], Sung-Hoon Cho[3], and Yong Gyu Choi[1]*

[1]Department of Materials Science and Engineering, Korea Aerospace University, Goyang 10540, Korea
[2]Division of Advanced Materials Engineering, Kongju National University, Cheonan 31080, Korea
[3]E-Hwa Industrial Co. Ltd., Hongcheon 25117, Korea

Retroreflection of vehicle headlights, as induced by spherical glass beads, is a key optical phenomenon that provides road-surface markings with greatly enhanced visibility, thus better securing a driver's safety in the nighttime as well as in unclear daytime. Retroreflectance of glass beads is a quite sensitive function of their refractive index, so that measurement of the refractive index of glass specifically in the shape of spherical beads needs to be performed within a reasonable uncertainty that is tolerable for road-marking applications. The Becke line method has been applied in assessing refractive index of such glass beads as *e.g.* an industrial standard in the Republic of Korea; however, the reference refractive-index liquids are not commercially available these days for refractive index greater than 1.80 due to the toxicity of the constituent materials. As such, high-refractive-index glass beads require an alternate method, and in this regard we propose a practically serviceable technique with uncertainty tantamount to that of the Becke line method: Based on comparison of calculated and measured retroreflectance values of commercial glass beads, we discover that their refractive index can be determined with reasonable precision via the retroreflectance measurement. Specifically, in this study the normalized retroreflectance originating from a single glass sphere is computed as a function of refractive index using the Fresnel equations, which is then validated as coinciding well with retroreflectance values measured from actual specimens, *i.e.* glass-bead aggregates. The uncertainties involved are delineated in connection with radius and imperfections of the glass beads.

Keywords : Glass beads, Road surface marking, Refractive index, Retroreflection, Fresnel equations
OCIS codes : (120.4800) Optical standards and testing; (120.5700) Reflection; (160.2750) Glass and other amorphous materials; (160.4670) Optical materials

I. INTRODUCTION

Visibility of road-surface markings is a critical safety issue, and in this regard the retroreflection of a vehicle's headlight beams from glass beads is one of the key enablers that improve visibility especially to drivers [1]. For this purpose, glass beads meeting basic requirements associated with refractive index and size need to be installed in practice [2]. It is well recognized that the retroreflectivity of glass beads is quite sensitive to their refractive index (n) as well as the refractive index of the surrounding medium, *i.e.* air or water in most cases, so that n of the glass beads should be carefully chosen to maximize the visibility of a given road-surface marking [3]. Specifically, it has been experimentally verified that the retroreflectance (R_A) of glass beads for use in road-marking applications is maximized at $n \approx 1.9$ and $n \geq 2.4$ (exact values not known) for dry and wet conditions, respectively [4, 5]. As such, in recent days high-n glass beads with $n \geq 1.8$ have been commercialized, which necessitates that their n values be evaluated, preserving the as-received shape of the glass beads within uncertainty limits that the

Color versions of one or more of the figures in this paper are available online.

related fields would require. It is noteworthy that the Becke line method, which has been employed as a standard technique for measuring n of glass beads, normally provides an uncertainty of ±0.05 in n for such beads. In the Becke line method, a Becke line originating from the difference of n between the glass beads under inspection and the surrounding medium is able to indicate n of the beads, and therefore this method requires reference refractive-index liquids that are commercially available. However, those liquids with $n \geq 1.8$ cannot be purchased due to the toxicity of their constituents such as As and Br. This situation means that we need to contrive another method capable of measuring the refractive index of tiny spheres of glass usually less than 1 mm in diameter. The so-called secondary-rainbow method exploits a circular pattern formed as a result of refraction and reflection of a laser beam by a spherical and transparent glass bead [6]. This method is known to give reasonably accurate n values, but requires a complicated experimental setup. In addition, because each glass bead makes its own unique secondary rainbow, n values thus measured should be treated statistically to present an average n for a given set of glass beads. A few other studies have also proposed methods relevant to measuring n of glass beads [7-12]. However, these methods were all performed in a laboratory setting, which still demanded measurements using complicated experimental setups and subsequent calculations. Moreover, these methods were inappropriate for glass beads with sub-millimeter diameters.

Based on the above considerations, in this study we have aimed to devise a facile and reliable method for n measurement of high-n glass beads, $n \geq 1.8$ in particular,

that excludes not only harmful chemicals but also such intricate setups as mentioned above. With this in mind, we calculated R_A as a function n of an arbitrary single glass sphere based on the Fresnel equations, and then measured R_A values of a group of commercially available glass beads with different n values. The calculated and measured R_A values were carefully compared in consideration of extrinsic factors such as diameter and roundness as well as imperfections like bubbles and cracks. In addition, sources of the uncertainties involved in the present method are delineated in comparison to existing methods.

II. MATERIALS AND METHODS

Available in this study were eleven different batches of commercial glass beads with refractive indices ranging from approximately 1.5 to approximately 2.4, as listed in Table 1. Their n values were verified, when possible, via the Becke line method using reference refractive-index fluids (Refractive Index Liquids, Cargille Laboratories) under white-light irradiation. For glass beads with n values greater than 1.8, to which the Becke line method cannot be applied, the supplier-specified values were utilized without further investigation (see Table 1 again). Note that batch **F** was confirmed to possess $n = 1.88$ by using high-refractive-index fluids ($n \geq 1.80$) purchased and stored prior to cessation of their sale. Consequently, their R_A values were measured using a commercial instrument (Handheld Retro-reflectometer 932; Roadvista) in accordance with the related standardized methods [13-15]. The retroreflectance of the instrument was calibrated with a black plate, and angles

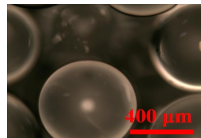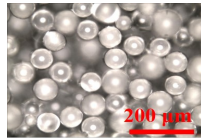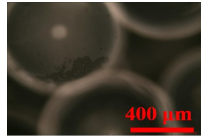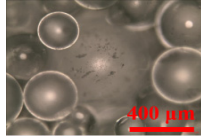TABLE 1. Refractive index, radius, and appearance of the prepared glass-bead batches
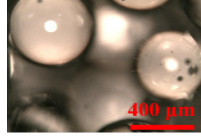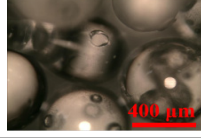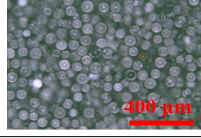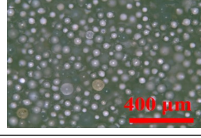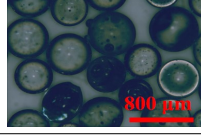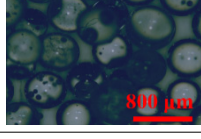
Glass bead batch	n	Radius (μm)	Optical microscopic image	Remarks
A	1.70	313 ± 46		- Negligible amount of internal bubbles - Reasonably acceptable surface condition
B	1.93 (supplier-specified)	39 ± 2		- Almost no internal bubbles - Reasonably acceptable surface condition - Relatively good sphericity
C	1.52	481 ± 24		- Considerable amount of bubbles - Reasonably acceptable surface condition
D	1.58	246 ± 49		- Moderate surface condition - Non-uniform sphericity - Negligible amount of bubbles

TABLE 1. Refractive index, radius, and appearance of the prepared glass-bead batches (Continue)

Glass bead batch	n	Radius (μm)	Optical microscopic image	Remarks
E	1.63	661 ± 30		- Considerable amount of bubbles - Acceptable sphericity and surface condition
F	1.88	175 ± 80		- Moderate sphericity and defects on surfaces - Negligible amount of bubbles
G	1.67	284 ± 66		- Poor surface condition - Non-uniform sphericity - Considerably large amount of bubbles
H*	1.9 (supplier-specified)	40 ± 4		- Moderate amount of bubbles - Acceptable surface condition and sphericity
I*	2.4 (supplier-specified)	38 ± 5		- Moderate amount of bubbles - Reasonably acceptable surface condition
J*	1.9 (supplier-specified)	289 ± 47		- Moderate amount of bubbles and defects on surfaces - Reasonably uniform sphericity
K	Unknown	270 ± 28		- Moderate amount of bubbles and defects on surfaces - Reasonably uniform sphericity

*Refractive index of these glass bead batches was noted to the first decimal place.

for light entrance and observation were fixed to be 0 and 0.2 degrees respectively during the measurements. Each glass batch was sampled for 27 specimens for R_A measurement in an effort to improve the statistical reliability of the obtained R_A values; the minimum and maximum were discarded, and the remaining 25 values were averaged.

III. CALCULATION OF THE RETRO-REFLECTANCE OF A GLASS BEAD

To numerically correlate n and R_A for a glass bead, we take into consideration an optically transparent dielectric solid that is perfectly spherical in shape, as displayed in Fig. 1. We consider illumination by tightly spaced multiple rays propagating parallel to the reference horizontal line,

i.e. the optical axis. Upon interaction with the glass sphere, the retroreflection angle (θ) of such optical rays, defined as in Fig. 1, is given as a function of incidence angle (a) and internal reflection angle (b) in Eq. 1, as below [16]:

$$\theta = \pi + 2a - 4b, \tag{1}$$

where a and b are related via Snell's Law for any given n of the glass sphere. In our numerical assessment, the θ values are calculated for every 0.01 degree step in a for varying n values. Specifically, in the present numerical modeling we consider only the beams that experience specular reflection from the backside interface of the glass sphere. Light beams specular-reflected several times inside can also contribute to retroreflected beams; however, the relative intensity of these beams is assumed to be too weak to alter the overall efficiency of retroreflection.
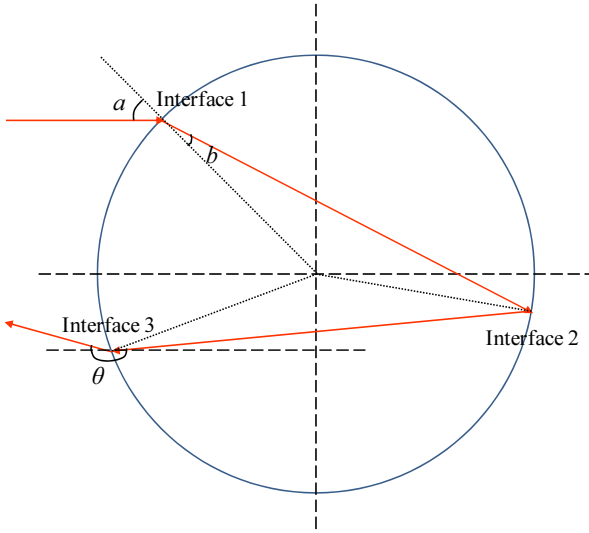
FIG. 1. Schematic drawing of a single glass bead hosting one internal specular reflection at the backside interface.

FIG. 2. Correlation between a and θ plotted for differing refractive index of a glass sphere.

As shown in Fig. 2, when n of the glass bead is smaller than 2.0, the retroreflection angle decreases in the low-a range, then increases with increasing angle of incidence, featuring a minimum θ value in the middle. On the other hand, when n is greater than or equal to roughly 2.0, the retroreflection angle monotonically increases with increasing a across the entire a range. In addition, notably, the number of beams heading toward θ close to 180°, which satisfies the retroreflection condition, turns out to depend sensitively on n of the glass bead; when $n \approx 1.9$, the number of retroreflected beams appears to be maximized, compared to other values of refractive index. It is noteworthy, however, that R_A depends not only on the number of the retroreflected beams but also on their relative intensity. This implies that we need to take into account changes in intensity for each beam under consideration to numerically find the correlation between n and R_A more accurately. To obtain the intensity of retroreflected beams, the reflectivity (r_s) and transmissivity (t_s) of s-polarized light are calculated using the Fresnel equations, Eqs. (2) and (3). Likewise, the reflectivity (r_p) and transmissivity (t_p) of p-polarized light are calculated using Eqs. (4) and (5) [17]:

$$r_s = \frac{n_i \cos \theta_i - n_t \cos \theta_t}{n_i \cos \theta_i + n_t \cos \theta_t},$$ (2)

$$t_s = \frac{2 n_i \cos \theta_i}{n_i \cos \theta_i + n_t \cos \theta_t},$$ (3)

$$r_p = \frac{n_t \cos \theta_i - n_i \cos \theta_t}{n_t \cos \theta_i + n_i \cos \theta_i},$$ (4)

$$t_p = \frac{2 n_i \cos \theta_i}{n_i \cos \theta_t + n_i \cos \theta_i},$$ (5)

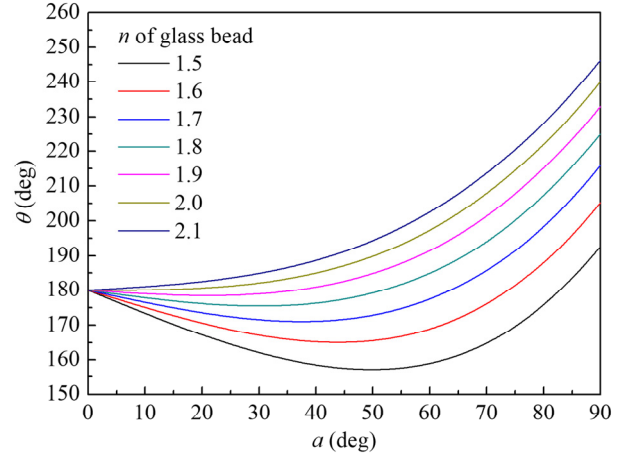where n_i and n_t are the refractive index of the surrounding medium (air in this particular case) and the glass bead respectively. Symbols θ_i and θ_t correspond to the angles of incidence and transmission respectively. It must be noted that both θ_i and θ_t should be equated differently at each interface in Fig. 1: At Interface **1**, $\theta_i = a$ and $\theta_t = b$. At Interface **2**, we require specular reflection, so $\theta_i = \theta_t = b$. At Interface **3**, the reflected beam escapes from the glass bead in a way that satisfies $\theta_i = b$ and $\theta_t = a$. Reflectance (R) and transmittance (T) can be obtained using Eqs. (6) and (7), respectively; however, polarization-averaged (or unpolarized) reflectivity (r) and transmissivity (t) are required:

$$R = r^2,$$ (6)

$$T = \frac{n_t \cos \theta_t}{n_i \cos \theta_i} t^2.$$ (7)

In this study, we disregard any polarization of the optical beams that interact with the glass bead; all beams are treated as unpolarized light. As a result, we obtain Eqs. (8) and (9) as follows:

$$r^2 = r_s^2 + r_p^2,$$ (8)

$$t^2 = t_s^2 + t_p^2.$$ (9)

Now, accommodating the abovementioned parameters, the relative intensity of each optical ray (I_r) is calculated using Eq. (10):

$$I_r = T_1 R_2 T_3 \cos a.$$ (10)

T_1 and T_3 indicate the transmittance of the optical ray at Interfaces **1** and **3** respectively, while R_2 corresponds to the reflectance at Interface **2**. As displayed in Fig. 3, it is

seen that the I_r values for the retroreflected rays, *i.e.* $\theta \approx$ 180°, are conspicuously sensitive to n of the glass bead. To obtain a more straightforward and quantitative dependence of retroreflectance for a desired θ slot, we derive R_A from summing the I_r values falling inside the θ slot, and subsequently normalize to the maximum value. Figure 4 reveals, as expected, that the maximum R_A appears at different n values, when the slot width, viz. observation angle, is changed. More specifically, when the observation angle is narrowed the corresponding R_A profile tends to narrow, and at the same time shift toward the high-n side.
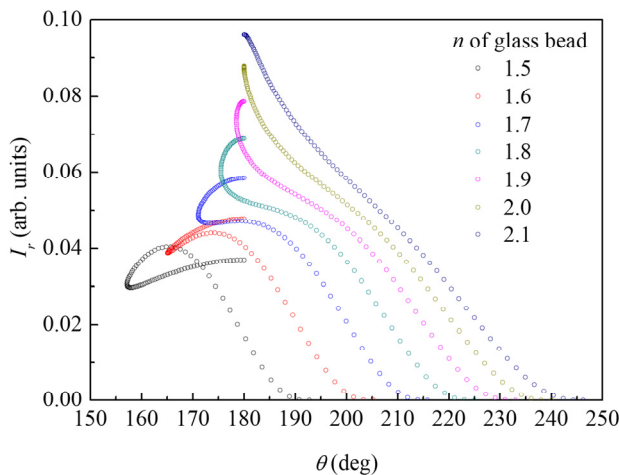

FIG. 3. Correlation between θ and I_r for different n of a glass sphere.
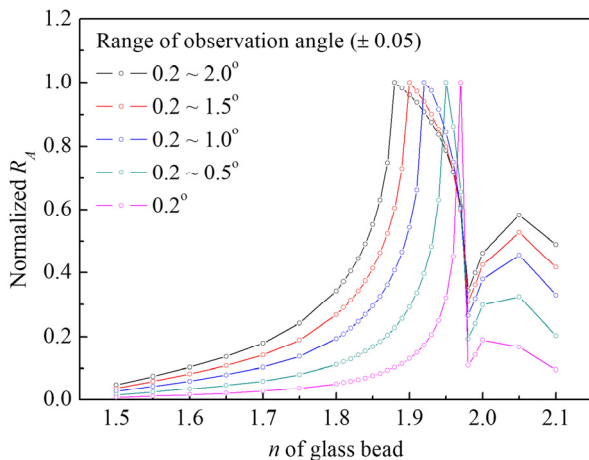

FIG. 4. Normalized R_A values plotted as a function of n of a glass sphere for different ranges of observation angle. Here, *observation angle* denotes the angle between the optical axis and the direction in which the photodetector in the instrument deployed in this study is located. Note that the minimum observation angle of the instrument is 0.2°, and the active area of the photodetector in the instrument corresponds to an angle range of 0.05°, so that we introduce an uncertainty of 0.05° for each observation angle under consideration.

IV. COMPARISON BETWEEN THE CALCULATED AND MEASURED RETROREFLECTANCE VALUES

As stated above, a single absorption-free glass sphere with no refractive-index dispersion is taken into account in the present calculation. Therefore, those calculated retro-reflectance curves need to be compared to the measured ones to ensure the conformity of our approach in evaluating refractive index of a given glass-bead batch via measurement of retroreflectance. The refractive indices of the glass-bead batches vary from ~1.5 to ~2.4, covering a wide enough range for practically available glass-bead products. Here it should be noted that each of the calculated R_A curves is normalized with regard to a maximum value in each curve, so that the measured R_A values also need to be normalized, and a glass batch for which the refractive index is already known should serve as a reference standard. Displayed in Fig. 5 are R_A values calculated in the case of an observation angle of $0.2 \pm 0.05°$, which is supposed to be identical to the measurement conditions of the instrument utilized in this study. Here, glass-bead batch **B** is designated as a reference, and its measured retroreflectance is set to coincide with the calculated R_A value at its refractive index. We rationalize that glass-bead batch **B** is able to serve as a proper reference in consideration of its members' radius, sphericity and appearance.

One can notice from Fig. 5 that the measured R_A values appear quite close to the calculated R_A curve, except for batches **G** and **J**, for which the mismatch is relatively more significant. Since n values for batches **H**, **I** and **J** are provided to us to the first decimal place at best, the uncertainty involved in the R_A comparison should be higher compared to the remaining batches for which n is confirmed to the second decimal place. As such, the
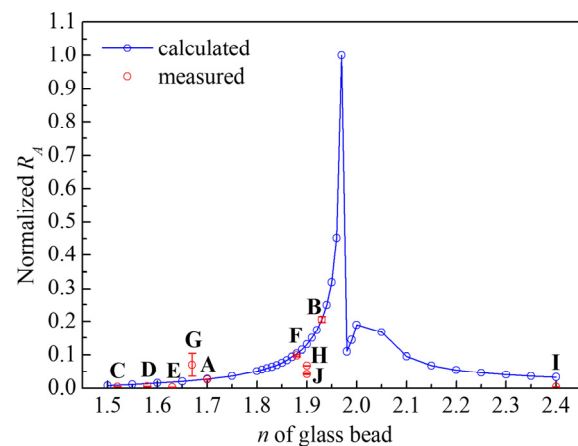

FIG. 5. Comparison of calculated and measured R_A values. The observation angle is fixed to $0.2 \pm 0.05°$ in this plot. Refer to Table 1 for the letters indicating the glass-bead batches. Note that glass-bead batch **K** is not presented, because its refractive index is unknown.

discrepancy observed for batch **G** is worth mentioning: It can be intuitively envisaged that retroreflectance of any given commercial glass beads is subject to not only refractive index but also many other factors concerning measurement conditions and the quality of the glass beads [18]. First, the measured R_A tends to decrease with increasing radius of the glass beads under inspection, as the number of glass beads residing within the illuminated area decreases. Second, the measured and calculated R_A values would exhibit nontrivial difference when the sphericity (roundness) of the beads deteriorates. As mentioned above, a perfectly spherical glass bead is employed in the calculation of R_A in this study, so the measured R_A would be lower for beads of poor sphericity. Third, both internal and surface defects (*e.g.* pores and cracks respectively) present in glass beads are supposed to deteriorate their efficiency of retroreflection. It is worthwhile noting that industry standards claim some regulations associated with identification of such defects, the fraction of defective glass beads, and the radius range of glass beads that needs to be sieved, if necessary [13]. Diffuse reflection is known to contribute to the intensity of a retroreflected beam as well [19, 20]. Fourth, color and refractive-index dispersion of glass beads deserve our attention. Glass beads free of defects normally reveal no color induced by scattering; however, if glass has a narrowed band-gap energy, then it is colored, and features corresponding absorptions over the visible wavelengths. Note that compositional adjustments made to increase refractive index above ~1.8 are likely to decrease the band-gap energy [21]. As a result, especially in the case of high-n glass beads, transmittance is deteriorated on the short-wavelength side, resulting in decrease of measured R_A values.

Along with the inherent deficiency due to simplification associated with the present calculations of R_A values, the majority of the abovementioned extrinsic attributes that cause deviations between calculated and measured R_A values are supposed to be mitigated down to an acceptable degree with the help of a properly chosen experimental reference. Specifically, a good reference needs to represent on average the respective glass-bead batches under observation, in terms of size and quality. In an effort to quantitatively assess mismatch between the two values, the R factor is adopted as follows [22]:

$$R = \frac{\sum (x_m - x_c)}{\sum x_m^2}, \tag{11}$$

where x_m and x_c stand for the experimentally measured value and the theoretically calculated value respectively. Note that the R factor is obtained from glass-bead batches, except for **H**, **I** and **J**, based on the reason stated above. Taking a look at Fig. 5 again, one can notice that batch **G** reveals an exceptionally large discrepancy between calculated and measured R_A values. Including batch **G**, the R factor turns out to be 0.05; this value decreases drastically down to 0.01 when excluding bead **G**. As shown in Table 1, in batch **G** the glass beads are remarkably poorer in terms of interior, surface, and roundness, thus differentiating this batch from the others. In this regard, it seems understandable why batch **G** reveals the most significant deviation. Interestingly, however, the measured R_A for batch **G** is higher than its calculated counterpart, the reason for which remains unresolved.

V. EVALUATION OF REFRACTIVE INDEX USING MEASURED RETROREFLECTANCE

Provided that the as-measured retroreflectance values are adequately normalized against a standard reference and then compared to the calculated R_A curve, refractive index can be estimated. Summarized in Table 2 are the refractive indices of the glass-bead batches employed in this study. Here, it needs to be emphasized that the related industrial

TABLE 2. Refractive indices determined by the Becke line method and the retroreflectance method proposed in this study

Glass bead batch	n (Becke line method)	n (retroreflectance method)	Difference
A	1.70	1.73	0.03
B	1.93*	1.93 (set as reference)	
C	1.52	<1.50	>0.02
D	1.58	<1.50	>0.08
E	1.63	<1.50	>0.13
F	1.88	1.87	0.01
H	1.9*	1.84	0.06
I	2.4*	>2.4 or <1.6	Not determinable
J	1.9*	1.77	0.13
K	Unknown	1.88	Not available

*Not measured by Becke line method, but specified by supplier.

standards normally require uncertainty tantamount to ±0.05 in assessment of refractive index using the Becke line method. As such, the present retroreflectance method provides a reasonably accurate refractive index for glass beads, in particular when $n \geq 1.80$, due to the relatively steep changes of the R_A curve (refer to Fig. 5). As described above, n for some glass-bead batches is less accurately known, so the corresponding differences observed here are supposed to be larger: 0.06 and 0.13 for batches **H** and **J** respectively. In addition, batch **K**, for which n is not available from the manufacturer, is estimated to have $n = 1.88$, being closer to 1.9 than 2.4 among commercial glass beads for road-marking applications. Now, our concern is focused on bead **I** with $n = 2.4$, because of ambivalence in estimating its refractive index. Due to the unique lineshape of the calculated R_A curve, which peaks between 1.9 and 2.0, bead **I** is determined to possess n greater than 2.4 or smaller than 1.6 just based on its measured R_A value. It is plausible, though, that the Becke line method can discriminate whether its n is greater than 1.80. Therefore, its n can be identified more accurately by combining both methods. Judging from the results described in Table 2 and Fig. 5, the retroreflectance method proposed in this study seems to work well for high-n glass beads, complementing the Becke line method. Retroreflectance also depends on the refractive index of the medium surrounding the glass beads. Under wet conditions, glass beads are immersed in water (normally rainfall), and correspondingly their retroreflectance changes. Following the methodology proposed in this study, the R_A curves for wet conditions can be derived and then compared to the measured R_A values. This is to be described in a forthcoming paper with a special emphasis paid to enhancing the accuracy level of the current retroreflectance method [23].

VI. SUMMARY

In an effort to devise a facile and reliable method for assessing the refractive index of commercial-grade glass beads for road-marking applications, we calculated retro-reflectance values of a single glass sphere as a function of its refractive index based on the Fresnel equations. We measured retroreflectance for commercially available glass beads with different n values (eleven in total), using a handy portable commercialized instrument. The measured retroreflectance values were then thoroughly compared to the calculated ones. Even though our calculation model is relatively simple, the refractive index of practical glass beads can be assessed within a reasonable uncertainty, tantamount to that of the Becke line method based on comparison of calculated and measured retroreflectance values. Attributes responsible for the observed mismatches are identified, and the accuracy of the present retro-flectance method would be improved further when employing retroreflectance values measured under wet conditions.

REFERENCES

1. L. A. Ivanov, D. V. Kiesewetter, N. N. Kiselev, V. I. Malyugin, and V. A. Slugin, "Measurement of retroreflection by glass beads for road marking," Proc. SPIE **6251**, 62510U (2006).
2. T. Grosges, "Retro-reflection of glass beads for traffic road stripe paints," Opt. Mater. **30**, 1549-1554 (2008).
3. J. T. Lee, T. L. Maleck, and W. C. Taylor, "Pavement marking material evaluation study in Michigan," ITE J. Inst. Transp. Eng. **69**, 44-51 (1999).
4. T. Schnell, F. Aktan, and Y. C. Lee, "Nighttime visibility and retroreflectance of pavement markings in dry, wet, and rainy conditions," Transp. Res. Rec. **1824**, 144-155 (2003).
5. D. M. Burns, T. P. Hedblom, and T. W. Miller, "Modern pavement marking systems: Relationship between optics and nighttime visibility," Transp. Res. Rec. **2056**, 43-51 (2008).
6. H. Fuquan, L. Shangying, and W. Shaomin, "The refractive index measurement of high refractive index glass beads," Acta Photon. Sin. **30**, 753-756 (2001).
7. F. Sarcinelli, R. Pizzoferrato, and F. Scudieri, "Study of the refractive index of microscopic glass beads by light-refraction analysis," Appl. Opt. **36**, 8999-9004 (1997).
8. J. L. Hand and S. M. Kreidenweis, "A new method for retrieving particle refractive index and effective density from aerosol size distribution data," Aerosol. Sci. Technol. **36**, 1012-1026 (2002).
9. A. Leblance-Hotte, R. St-Gelais, and Y.-A. Peter, "Opto-fluidic device for high resolution volume refractive index measurement of single cell," in *Proc. 16th International Conference on Miniaturized Systems for Chemistry and Life Sciences* (Japan, Oct. 2012), pp. 1330-1332.
10. T. Yamaguchi, "Refractive index measurement of high refractive index glass beads," Appl. Opt. **14**, 1111-1115 (1975).
11. R. W. Spinrad and J. F. Brown, "Relative real refractive index of marine microorganisms: a technique for flow cytometric estimation," Appl. Opt. **25**, 1930-1934 (1986).
12. S.-Y. Li, S. Qin, D.-H. Li, and Q.-H. Wang, "Using a laser source to measure the refractive index of glass beads and Debye theory analysis," Appl. Opt. **54**, 9688-9694 (2015).
13. *Glass beads for traffic paint*, KS L 2521, Korean Standard Association, Seoul (2017).
14. *Standard test method for measurement of retroreflective signs using a portable retroreflectometer at a 0.2 degree observation angle,* ASTM E1709-16e1, ASTM International, Pennsylvania (2016).
15. *Standard test method for measurement of retroreflective signs using a portable retroreflectometer at a 0.5 degree observation angle,* ASTM E2540-16, ASTM International, Pennsylvania (2016).

16. M. D. Stoudt and K. Vedam, "Retroreflection from spherical glass beads in highway pavement markings. 1: Specular reflection," Appl. Opt. **17**, 1855-1858 (1978).

17. E. Hecht, *Optics*, 4th ed. (Addison-Wesley, New York, 2002), Chapter 4.

18. G. Zhang, J. E. Hummer, and W. Rasdorf, "Impact of bead density on paint pavement marking retroreflectivity," Transp. Eng. J. ASCE **136**, 773-781 (2010).

19. K. Vedam and M. D. Stoudt, "Retroreflection from spherical glass beads in highway pavement markings. 2: Diffuse reflection (a first approximation calculation)," Appl. Opt. **17**, 1859-1869 (1978).

20. D. Héricz, T. Sarkadi, G. Erdei, T. Lazuech, S. Lenk, and P. Koppa, "Simulation of small- and wide-angle scattering properties of glass-bead retroreflectors," Appl. Opt. **56**, 3969-3976 (2017).

21. N. M. Ravindra, P. Ganapathy, and J. Choi, "Energy gap-refractive index relations in semiconductors-An overview," Infrared Phys. Technol. **50**, 21-29 (2007).

22. S. Y. Shin, B.-K. Cheong, and Y. G. Choi, "Local structural environments of Ge doped in eutectic Sb-Te film before and after crystallization," J. Phys. Chem. Solids **117**, 81-85 (2018).

23. S. Y. Shin, J. I. Lee, W. J. Chung, and Y. G. Choi, "Correlations between refractive index and retroreflectance of glass beads for use in road-marking applications under wet conditions," Curr. Opt. Photon. **3**, 423-428 (2019).